The Journal of Immunology

RESEARCH ARTICLE | JULY 15 2017

EBV Infection Empowers Human B Cells for Autoimmunity: Role of Autophagy and Relevance to Multiple Sclerosis FREE

Elena Morandi; ... et. al

J Immunol (2017) 199 (2): 435–448.
https://doi.org/10.4049/jimmunol.1700178

EBV Infection Empowers Human B Cells for Autoimmunity: Role of Autophagy and Relevance to Multiple Sclerosis

Elena Morandi,* S. Anwar Jagessar,† Bert A. 't Hart,†,‡,1 and Bruno Gran*,§,1

The efficacy of B cell depletion therapy in multiple sclerosis indicates their central pathogenic role in disease pathogenesis. The B lymphotropic EBV is a major risk factor in multiple sclerosis, via as yet unclear mechanisms. We reported in a nonhuman primate experimental autoimmune encephalomyelitis model that an EBV-related lymphocryptovirus enables B cells to protect a proteolysis-sensitive immunodominant myelin oligodendrocyte glycoprotein (MOG) epitope (residues 40–48) against destructive processing. This facilitates its cross-presentation to autoaggressive cytotoxic MHC-E–restricted $CD8^+CD56^+$ T cells. The present study extends these observations to intact human B cells and identifies a key role of autophagy. EBV infection upregulated APC-related markers on B cells and activated the cross-presentation machinery. Although human MOG protein was degraded less in EBV-infected than in uninfected B cells, induction of cathepsin G activity by EBV led to total degradation of the immunodominant peptides $MOG_{35–55}$ and $MOG_{1–20}$. Inhibition of cathepsin G or citrullination of the arginine residue within an LC3-interacting region motif of immunodominant MOG peptides abrogated their degradation. Internalized MOG colocalized with autophagosomes, which can protect from destructive processing. In conclusion, EBV infection switches MOG processing in B cells from destructive to productive and facilitates cross-presentation of disease-relevant epitopes to $CD8^+$ T cells. ***The Journal of Immunology*****, 2017, 199: 435–448.**

Multiple sclerosis (MS) is a chronic demyelinating immune-mediated disease of the CNS characterized by inflammatory and neurodegenerative changes in the brain and spinal cord. Strong evidence suggests that B cells have a central pathogenic role in MS pathogenesis and progression. First, B cell depletion with anti-CD20 mAbs is effective in reducing disease activity in both relapsing and progressive forms of MS (1). Second, the presence of oligoclonal bands of Igs in the cerebrospinal fluid is a sensitive biomarker of MS and has been associated with MS activity, progression, and prognosis (2). Third, the presence of B cell aggregates within tertiary lymphoid follicles has been detected in the meninges of patients with advanced MS (3). B cells are thought to contribute to MS pathogenesis through Ag presentation to T cells and the production of Abs and cytokines (4).

We focused our research on the processing and presentation by B cells of the autoantigen myelin oligodendrocyte glycoprotein (MOG). Processing of exogenous protein autoantigens involves uptake into endosomes and partial degradation by endolysosomal proteases. Peptides of the appropriate length are generated, which are loaded within the endolysosomal compartment on HLA-II molecules for presentation to $CD4^+$ T cells (5). The sequence of events that leads to the processing and presentation of autoantigens in autoimmune diseases is still incompletely understood. Self-reactive T cells that have escaped central and peripheral tolerance are present in healthy subjects, indicating that further pathogenic steps are required for the emergence of autoimmunity. Infectious agents are thought to play an important role in triggering autoimmunity, through effects on both APC and lymphocytes (6).

The etiology of MS is still unknown. On the background of genetic susceptibility (7), both infectious and noninfectious environmental factors can modulate the risk of developing the disease. Among infectious factors, the lymphocryptovirus (LCV) EBV is the most strongly associated with MS. This virus infects human B cells in ~90% of the general population and virtually 100% of those with MS. Adults without evidence of remote infection by EBV appear not to develop MS, indicating that such infection may be a prerequisite for disease development (8). Several hypotheses have been proposed to explain how EBV infection could trigger MS: bystander damage, cross-reactivity due to molecular mimicry, activation of human endogenous retroviruses, and autoantigen presentation (9).

Evidence from a nonhuman primate (NHP) experimental autoimmune encephalomyelitis (EAE) model shows that the EBV-related LCV CalHV3–infected B cells play a critical role in the pathogenesis of the disease. The data show that the anti-CD20 mAb, which had a robust clinical effect, induced systemic

*Division of Clinical Neuroscience, University of Nottingham School of Medicine, Nottingham NG7 2UH, United Kingdom; †Department of Immunobiology, Biomedical Primate Research Centre, Rijswijk 2288, the Netherlands; ‡Department of Neuroscience, University Medical Center, University of Groningen, Groningen 9700, the Netherlands; and §Department of Neurology, Nottingham University Hospitals NHS Trust, Nottingham NG7 2UH, United Kingdom

[1]B.A.t.H. and B.G. contributed equally to this work.

ORCIDs: 0000-0002-8222-1514 (E.M.); 0000-0002-0036-5267 (B.A.t.H.); 0000-0001-6384-2342 (B.G.).

Received for publication February 2, 2017. Accepted for publication May 5, 2017.

This work was supported in part by unrestricted grants to B.G. from Sanofi Genzyme, Biogen, and Novartis. E.M. was supported by a Vice-Chancellor Scholarship for Research Excellence from the University of Nottingham.

Address correspondence and reprint requests to Dr. Bruno Gran, Nottingham University Hospitals NHS Trust, Department of Neurology - C Floor, South Block, Queen's Medical Center, Nottingham NG7 2UH, U.K. E-mail address: Bruno.Gran@nuh.nhs.uk

The online version of this article contains supplemental material.

Abbreviations used in this article: Arg, arginine; BAF, bafilomycin; B-LCL, B lymphoblastoid cell line; Cat, cathepsin; Cit, citrulline; CTRL, control; EAE, experimental autoimmune encephalomyelitis; FC, flow cytometry; LCV, lymphocryptovirus; LIR, LC3-interacting region; MBP, myelin basic protein; MFI, mean fluorescence intensity; MOG, myelin oligodendrocyte glycoprotein; MS, multiple sclerosis; NHP, nonhuman primate; ON, overnight; RAP, rapamycin; rh, recombinant human; rMFI, relative MFI; ROI, region of interest.

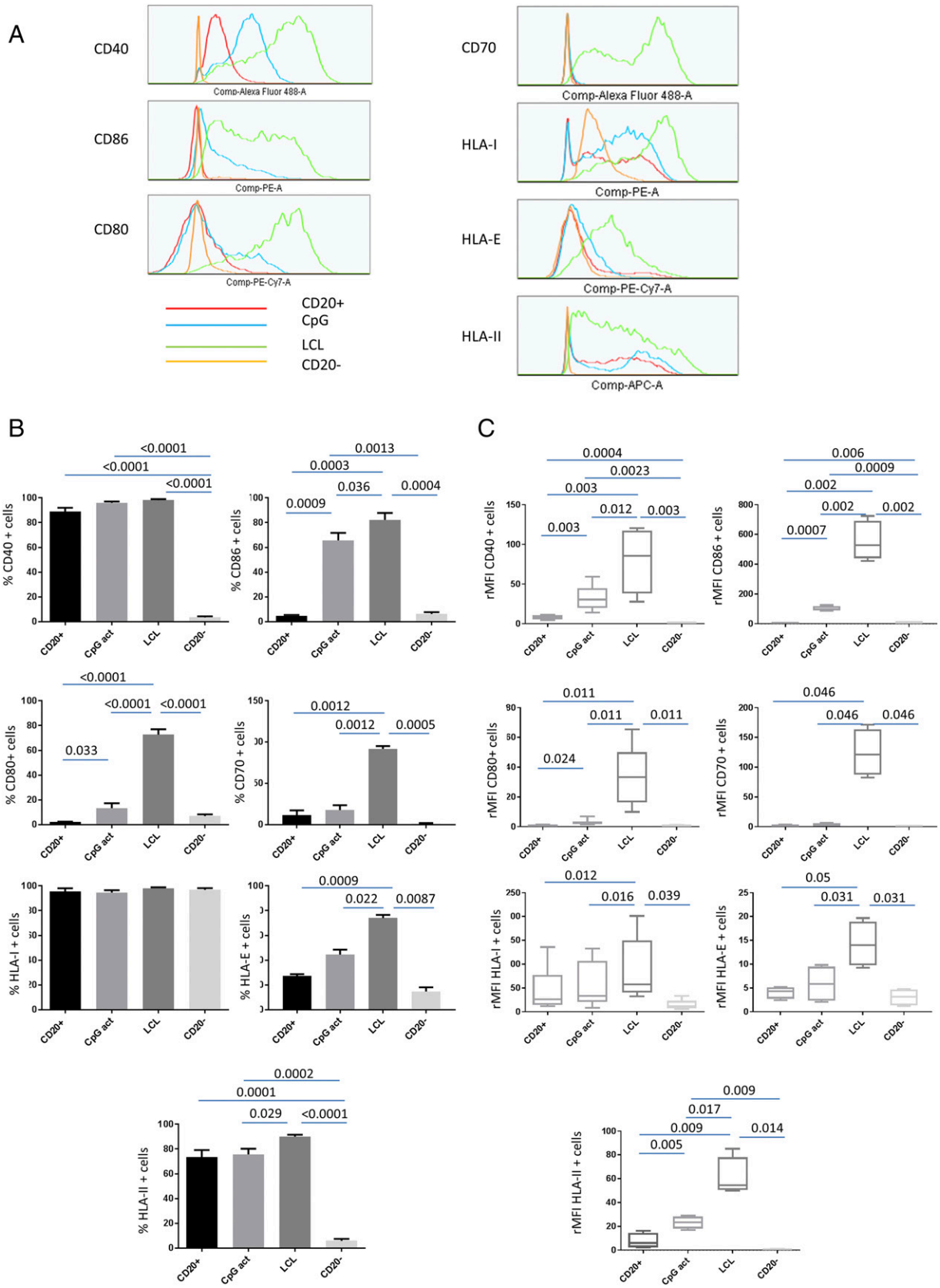

FIGURE 1. EBV increases Ag presentation–related markers of B cells. Isolated CD20$^+$ cells, CpG–activated CD20$^+$ cells, B-LCL, and CD20$^-$ cells were obtained from the same subjects. (**A**) One representative histogram overlay is shown for each marker CD40, CD86, CD80, CD70, HLA-I (A, B, C), HLA-E, and HLA-II (DR, DP, DQ). Dot-plot data are representative of $n = 8$ independent experiments from different donors showing the mean and the SEM of extracellular expression of (**B**) cells positive for each marker and (**C**) their rMFI ($n = 8$ pairing, repeated-measure one-way ANOVA with Greenhouse-Geisser correction).

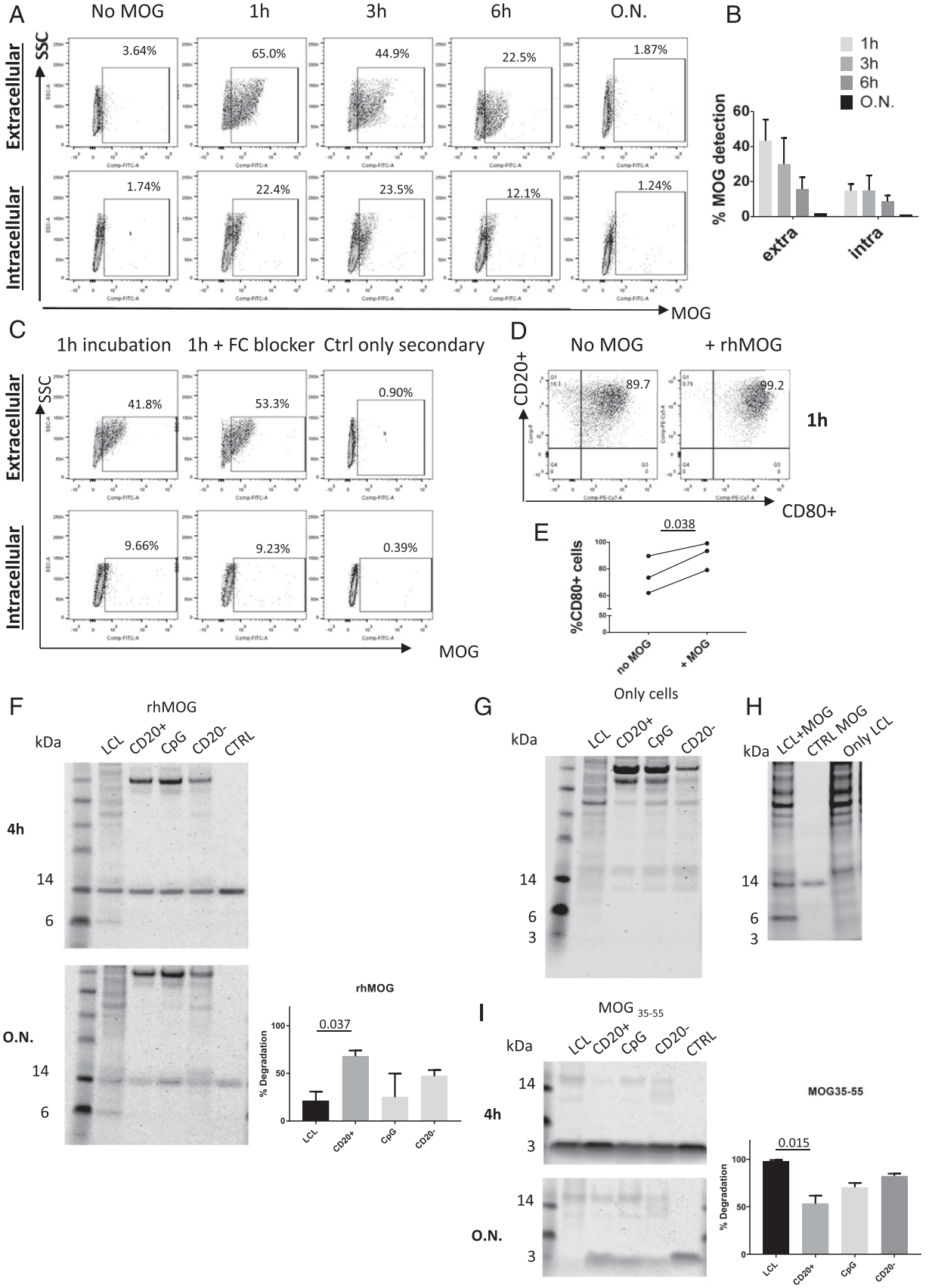

FIGURE 2. B-LCL bind and internalize rhMOG and can process rhMOG and $MOG_{35–55}$. (**A**–**C**) After incubation of B-LCL with rhMOG for 1, 3, 6 h, and ON, rhMOG can be detected extra- and intracellularly by FC with primary 8-18C5 anti-MOG Ab and secondary FITC-anti mouse IgG. (A) Dot-plot data are representative of $n = 3$ independent experiments from different donors summarized in (B). (C) The expression of rhMOG after 1 h incubation has also been detected in the presence of Fc blocker. The last panel represents the control of the staining with no primary anti MOG Ab. (**D** and **E**) After incubation of B-LCL with rhMOG, the expression of CD80 has been reported after 1 h. (D) Dot-plot data are representative of (*Figure legend continues*)

depletion of LCV, whereas treatment directed at B cell survival factors, such as anti-BLyS or anti-APRIL, which were only partially effective, did not reduce LCV viral load (10). LCV CalHV3 can influence the ability of B cells to process and present autoantigens to $CD4^+$ and $CD8^+$ T cells. The development of pathological and clinical manifestations of EAE (CNS inflammation and paralysis) in specific pathogen-free–bred mice requires the administration of human MOG as an emulsion with CFA (heat-killed mycobacteria emulsified with mineral oil), whereas in rhesus macaques and marmosets IFA (only the mineral oil) is sufficient. Interestingly, the infusion of autologous LCV-infected B cells prepulsed in vitro with the immunodominant $MOG_{34–56}$ peptide induced autoreactive T cell activation and meningeal inflammation in rhesus macaques (11) and marmosets (10). Specifically, LCV-infected B cells have a central role in the activation of highly pathogenic MHC-E restricted effector memory $CD8^+CD56^+$ CTLs, which upon activation with $MOG_{34–56}$ (the core epitope of the peptide is residues 40–48) can elicit MS-like pathology and disease. LCV infection activates the cross-presentation machinery in NHP B cells and prolongs the half-life of the CTL epitope. The fast proteolytic degradation of the Ag in the endolysosomal compartment is suppressed to enable translocation to the MHC class I loading pathway. B cells are thus enabled to cross-present the marmoset $MOG_{40–48}$ epitope (YRSPFSRVV) to $CD8^+$ T cells. Cathepsin (Cat)G has a leading role in the degradation of $MOG_{35–51}$, but citrullination of Arg46 makes the peptide completely resistant to proteolytic degradation in the rhesus monkey cell lysates (12). The arginine (Arg) to citrulline (Cit) substitution is a physiologically relevant modification of antigenic peptides, mediated by the enzyme peptidyl arginine deiminase, which can occur in autophagosomes that form in stressed B cells. Autophagosomes are implicated in cross-presentation and we have recently proposed that they may also play a role in protecting MOG peptides against destructive processing (13).

Having explored the above mechanisms in lysates of NHP lymphocytes (12), in the current study we focused on the effect of human EBV infection and autophagy in MOG processing by intact noninfected and EBV-infected human B cells. We used EBV-infected B lymphoblastoid cell lines (B-LCL) generated in vitro that represent a tissue culture model for human B cell transformation and virus latency (14). We found that 1) EBV infection increases Ag presenting cell–related markers on the surface of B cells; 2) EBV-infected cells can bind and internalize recombinant human (rh) MOG; 3) EBV infection reduces degradation of rhMOG, but leads to complete degradation of MOG peptides harboring immunodominant epitopes (destructive processing) due to increased activity of CatG; 4) citrullination of Arg residues in a putative LC3-interacting region (LIR) motif within epitopes protects immunodominant peptides from degradation (productive processing) mediating the association with autophagosomes; and 5) autophagy is directly involved in processing MOG peptides and is induced by EBV infection.

We propose a new mechanism by which EBV infection modulates the processing of a disease-relevant myelin autoantigen through autophagy. This could facilitate cross-presentation to CTLs that may be involved in MS induction and progression.

Materials and Methods

Study design

This is an experimental laboratory study performed with human peripheral blood samples. The study was designed to better understand the role of EBV infection in the processing of the MS-relevant autoantigen, MOG. Healthy subjects (n = 8, mean age = 40.1, SD = 10.7) were recruited among volunteers in the Division of Clinical Neuroscience at the University of Nottingham. All subjects provided informed consent as approved by the ethics review board. Study components were not predefined. The number of replicates for each experiment is indicated in *Results* and in the figure legends. Immunofluorescence experiments were not blinded, except for the acquisition of data at the microscope. All other studies (flow cytometry or protein gels) were performed without randomization or blinding. Infection of the cells with EBV and the handling of EBV-infected cells were performed following the University of Nottingham risk assessment protocols for biological agents.

Cell culture

Human PBMC were separated by density centrifugation using Histopaque (Sigma-Aldrich). $CD20^+$ B cells were purified by positive selection using a $CD20^+$ cell isolation kit (Miltenyi Biotec) according to the manufacturer's protocol. $CD20^-$ cells were also collected. The purity of the cells was checked by flow cytometry (FC) after each isolation, and the typical purity was >98% (Supplemental Fig. 1). Next, 10^6 $CD20^+$ isolated B cells were cultured in complete medium (RPMI 1640 with 10% FCS, 100 U penicillin-1 mg/ml streptomycin, 20 mM L-glutamine; all from Sigma-Aldrich) with 30 μg/ml CpG oligodeoxynucleotides 2006 (InvivoGen, sequence TCG TCG TTT TGT CGT TTT GTC GT) in 48-well plates for 24 h. Activation of $CD20^+$ cells was assessed using an anti-CD86 Ab by FC (Supplemental Fig. 1). For the establishment of B-LCL, 5–10 million of isolated PBMC were infected with supernatant from a B95.8 EBV–infected marmoset cell line (kindly donated by J. Brooks, Birmingham). The B95.8 supernatant was filtered on the PBMC pellet and PBMC mixed with the virus were incubated overnight (ON) at 37°C. Infected PBMC were cultured in 2 ml of CSA medium (complete medium + 1 μg/ml cyclosporin A from Sigma-Aldrich) in 24-well plates. After achieving the correct concentration, B-LCL were expanded using complete medium RPMI 1640. Once new B-LCL were established from each different donor, they were expanded in culture and used for further experiments.

MOG processing

rhMOG was purchased from Cambridge Bioscience and six synthetic peptides were purchased from Peptide 2.0 (Chantilly, VA). Peptides were derived from the human MOG sequence downloaded from the National Centre for Biotechnology Information protein database (http://www.ncbi.nlm.nih.gov/protein, Supplemental Table I). Modifications included substitution of the positively charged Arg residues on positions 41 and 46, and 4 and 13, for uncharged Cit. A total of 10^5 cells were incubated with 1 μg of rhMOG or 2 μg of MOG peptides for different time points as specified in the figure legends at 37°C in 96-well plates in complete medium with or without 0.1 mM Z-Gly-Leu-Phe-CMK CatG inhibitor (Sigma-Aldrich), 0.1 mM CatG inhibitor In2 (Calbiochem), or 0.01 mM E64 cysteine inhibitor (Sigma-Aldrich). When an Fc blocker was used, cells were incubated with MOG in the presence of 2.5 μg per 10^6 cells of human BD Fc Block (BD Biosciences). In CatG purified incubation, 5 mU/ml of human CatG (Sigma-Aldrich) was used. To modulate autophagy, cells were cultured either with 800 nM rapamycin (RAP; Calbiochem) for 4 h or 500 nM bafilomycin (BAF; Calbiochem) for 3 h or 10 mM 3-MA (Sigma-Aldrich) for 1 h.

Flow cytometry

Cells were washed two times with FACS buffer (PBS + 2% FCS) and incubated in the dark for 30 min at 4°C with Abs for CD20 (2H7), CD86 (2331), CD80 (L307.4), CD40 (5C3), CD70 (Ki-24), HLA- DR, DP, DQ (Tu39), HLA-ABC (G46-2.6), all from BD Biosciences and HLA-E (3D12) from BioLegend. Isotype controls were included and fluorescence minus one samples were used to set the gating. For detection of

n = 3 independent experiments from different donors, summarized in (E). (**F–I**) The presence of MOG can be detected with SDS gel. B-LCL, $CD20^+$, CpG–activated $CD20^+$, $CD20^-$ cells have been incubated with (F) rhMOG or (I) $MOG_{35–55}$ for 4 h or ON CTRL shows the protein incubated without the cells (rhMOG 14 kDa, $MOG_{35–55}$ 3 kDa). The right panel shows the mean with SEM of percentage degradation of rhMOG and $MOG_{35–55}$ after ON incubation in independent experiments calculated as described in *Materials and Methods* (n = 4, paired nonparametric Friedman test). Control gels show (G) B-LCL, $CD20^+$, CpG–activated $CD20^+$, $CD20^-$ cells incubated with no protein or peptide and (H) B-LCL incubated with or without rhMOG.

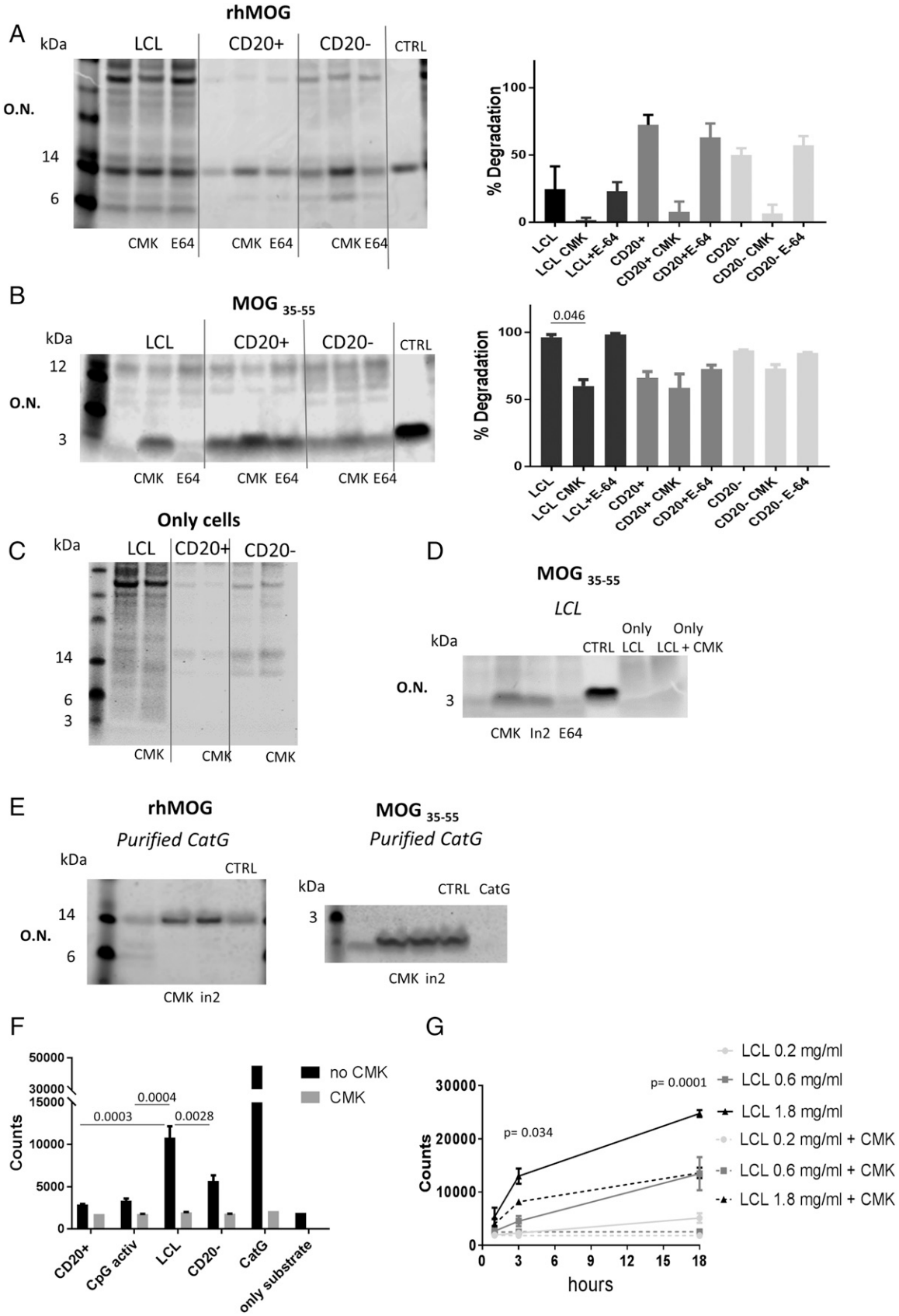

FIGURE 3. Involvement of CatG in proteolytic degradation of rhMOG and $MOG_{35–55}$. (**A**–**D**) Inhibition of (A) rhMOG (B) and $MOG_{35–55}$ degradation was performed incubating B-LCL, $CD20^+$, and $CD20^-$ cells ON with the proteins with or without CMK as CatG inhibitor and E64 as cysteine protease inhibitor. The right panel shows the mean with SEM of percentage degradation of (A) rhMOG and (B) $MOG_{35–55}$ after ON incubation in $n = 3$ independent experiments calculated as described in *Materials and Methods*. (C) A control gel shows B-LCL, $CD20^+$, CpG–activated $CD20^+$, $CD20^-$ cells incubated with or without CMK with no protein or peptide. (D) B-LCL were incubated ON with $MOG_{35–55}$ also with a second CatG inhibitor (In2). CTRL line represents the protein without cells, whereas the only B-LCL line shows the cells alone, and only B-LCL + CMK line shows the (*Figure legend continues*)

rhMOG, primary mouse IgG anti human MOG (8-18C5, kindly donated by Prof. Linington, University of Glasgow) and secondary FITC goat F(ab′)2 anti-mouse IgG (R&D Systems) were used. After incubation, cells were washed again two times with FACS buffer and fixed with fixation buffer (2% paraformaldehyde; BD Biosciences). For intracellular staining, cells were incubated for 20 min at 4°C with fix/perm buffer (BD Biosciences) to fix and permeabilize the cells; all washes were performed with perm/wash buffer (BD Biosciences). Cells were analyzed by FC using LSRII flow cytometer (BD Biosciences) and FlowJo software (version V10; Tree Star). Mean fluorescence intensity (MFI) raw values were divided by the MFI of the isotype control in each experiment to calculate relative MFI (rMFI) (relative to control).

Protein electrophoresis–based assay for processing experiments

Cells previously incubated with MOG protein or peptides for different time points (4 h, ON) were washed and frozen at −20°C. Samples with 4× loading buffer and 10× reducing agent (both Life Technologies) were loaded in NuPage Novex Bis-Tris precast protein gels, 4–12% (Life Technologies), and run at 100 V. Control (CTRL) was added loading only the MOG protein or peptides incubated without cells and only cells without the protein. Gels were stained with SimplyBlue SafeStain (Life Technologies) for 2–3 h and decolorized ON. The imaging was on an Odyssey scanner (LI-COR Biosciences) and quantified with Image Studio Lite version 4.0 software (LI-COR Biosciences). The percentage of degradation was calculated with the formula:

$$(\text{MOG incubated without cells} - \text{MOG incubated with cells})/\text{MOG incubated without cells}^{*}100.$$

Western blotting for LC3

Cell pellets were washed twice with PBS and lysed with radioimmunoprecipitation assay buffer (Sigma-Aldrich). Cell lysate was kept on ice for at least 30 min and centrifuged for 10 min at 8000 × *g* at 5°C. Bicinchoninic acid Protein Assay Kit (Thermo Scientific) was used for estimation of total protein content in the cell lysates. Color intensity was measured at 562 nm with a Benchmark Plus Spectrophotometer (Bio-Rad) and results analyzed with the Microplate Manager software. Equal amounts of lysates were resolved by a 12% denaturating SDS–PAGE (180 V, for 60 min). Proteins were transferred to polyvinylidene fluoride transfer membrane (GE Healthcare Life Sciences) (30 V, 90 min) and blocked in PBS-tween 2% BSA (Sigma-Aldrich) for 1 h. Blots were incubated ON with 1:1000 rabbit monoclonal anti human LC3A/B (D3U4C) Ab (Cell Signaling) and 1:10,000 mouse monoclonal anti human β-actin Ab (Sigma-Aldrich) at 4°C. They were then incubated with 0.06 μg/ml secondary 800CW donkey anti-rabbit IgG (H + L) and 680RD donkey anti-mouse IgG (H + L) (both from LICOR Biosciences) for 1 h at room temperature. The membrane was scanned with an Odyssey scanner (LI-COR Biosciences) at 700 nm (LC3) and 800 nm (actin), and band intensities were quantified with Image Studio Lite version 4.0 software (LI-COR Biosciences). To calculate LC3 relative expression, in each Western blot the band intensity for each cell group was divided by the band intensity of $CD20^+$ cells (considered as one).

CatG activity assay

CatG activity was measured in 200 μg/ml cell lysates in a total volume of 40 μl 160 mM Tris-HCL +1.6 M NaCl + 5 mM DTT (pH 7.4), and with or without the Z-Gly-Leu-Phe-CMK CatG inhibitor (0.1 mM; Sigma-Aldrich). After a preincubation of 30 min at 37°C, 10 μl of 200 μM Z-Gly-Gly-Arg-AMC substrate (Bachem, Bubendorf) was added. The total mixture was incubated for different time points (1, 3, 6 h, ON) at 37°C and fluorescence was measured with the Fluorostar OMEGA plate reader (BMG Labtech) at excitation wavelength 355 nm and emission 460 nm. As positive control, 5 mU/ml human CatG was used (Sigma-Aldrich). Values were normalized with the background measured with the substrate alone.

Immunofluorescence

Cells were washed with PBS with 2 mM EDTA and 0.5% BSA, and cytospins (50,000 cells per slide) were made with the Cytospin 4 Cytocentrifuge (Thermo Fisher Scientific). Cells were fixed and permeabilized for 30 min with cold 100% methanol, air dried, blocked with PBS + 5% FCS, and incubated with 1:100 rabbit monoclonal anti human LC3A/B (D3U4C) Ab (Cell Signaling), 1:100 mouse monoclonal anti human β actin Ab (Sigma-Aldrich), and 1:100 mouse IgG anti human MOG (8-18C5, kindly donated by Prof. Linington) in PBS+ 5% BSA ON at 5°C. Cells were washed three times with PBS and incubated with 1:1000 secondary CF 488A goat anti-rabbit IgG (H + L) Ab and CF 568 goat anti-mouse IgG (H + L) Ab (both from Sigma-Andrich) for 1 h at room temperature in PBS/1% BSA. After four final wash steps with PBS, coverslips were mounted with Vectashield mounting medium for fluorescence with DAPI (VECTOR). Imaging was performed with LSM880 confocal laser scanning microscope (Zeiss). A measure of LC3 expression was calculated using ImageJ (ImageJ-win64; National Institutes of Health). Thresholds were set to define regions of interest (ROIs) using the actin images. These ROIs were then used to analyze the expression of actin and LC3 within each particle (individual cell). The mean pixel intensity of $CD20^+$ cells was used as the denominator to normalize the expression of LC3 in the other cell types (the mean intensity of $CD20^+$ cells is considered as one). Different experiments were performed maintaining identical image acquisition settings and exposure times.

Statistics

GraphPad Prism 7 was used for all statistical analysis. Repeated one-way ANOVA was used for statistical comparisons in FC experiments. A paired nonparametric Friedman test was used for statistical comparison in quantification of gels. When more than one variable was considered, paired repeated two-way ANOVA was used. All statistical tests have been indicated in the figure legends. A p value ≤ 0.05 was considered significant.

Results

EBV infection upregulates Ag presentation–related markers

To study the effect of latent EBV infection in B cell processing and Ag presentation, we used B-LCL in comparison with other cell types derived from the same subjects: primary uninfected $CD20^+$ B cells, $CD20^-$ PBMC subfraction, and $CD20^+$ B cells activated ON with the TLR9 agonist CpG as a positive control (Supplemental Fig. 1). Previous reports indicate that CpG-activated B cells are capable of Ag cross-presentation (15, 16).

B-LCL are often used as prototypical APC in immunological assays. We measured the expression of principal Ag presentation–related markers to see if EBV can phenotypically induce their expression and increase cytokine production. EBV infection increased the expression of CD86, CD80, CD70, HLA-E, and class II (DR, DP, DQ) both in terms of rMFI (Fig. 1A, 1C) and the percentage of cells positive for the markers (Fig. 1B) as compared with all the other groups. CD40 was expressed by all the B cell groups, with higher rMFI in B-LCL (Fig. 1A, 1C). HLA class I (A, B, C) was expressed by all the different cell groups, with higher rMFI in B-LCL (Fig. 1A, 1C). B cells activated with CpG had an increased expression of CD40, CD86, CD80, and HLA-E compared with the primary uninfected $CD20^+$ cells, but the expression levels were significantly lower than in B-LCL.

In B-LCL, there was also an increased production of IFN-γ, but not TNF-α and IL-10, compared with other cell types (Supplemental Fig. 2).

These results confirm the previous indication (17, 18) that EBV infection leads to a potent activation of B cells, with increased expression of some of their Ag presentation markers.

B-LCL internalize and process rhMOG and $MOG_{35–55}$

MOG is an indispensable component of human myelin for the induction of chronic EAE in marmosets (19). The immunodominant

cells alone with CMK. (**E**) Purified human CatG was incubated ON with rhMOG and $MOG_{35–55}$ with or without CMK and In2. CatG line shows the purified CatG alone (n = 3, paired nonparametric Friedman test). (**F**) Activity measurement of CatG was performed in the absence or presence of CMK in the indicated cell lysates after ON incubation (n = 3, paired repeated-measure two-way ANOVA). (**G**) CatG contained in different concentration of B-LCL lysates (0.2, 0.6, 1.8 mg/ml) with or without CMK was measured after 1, 3 h and ON (n = 3, paired repeated-measure two-way ANOVA).

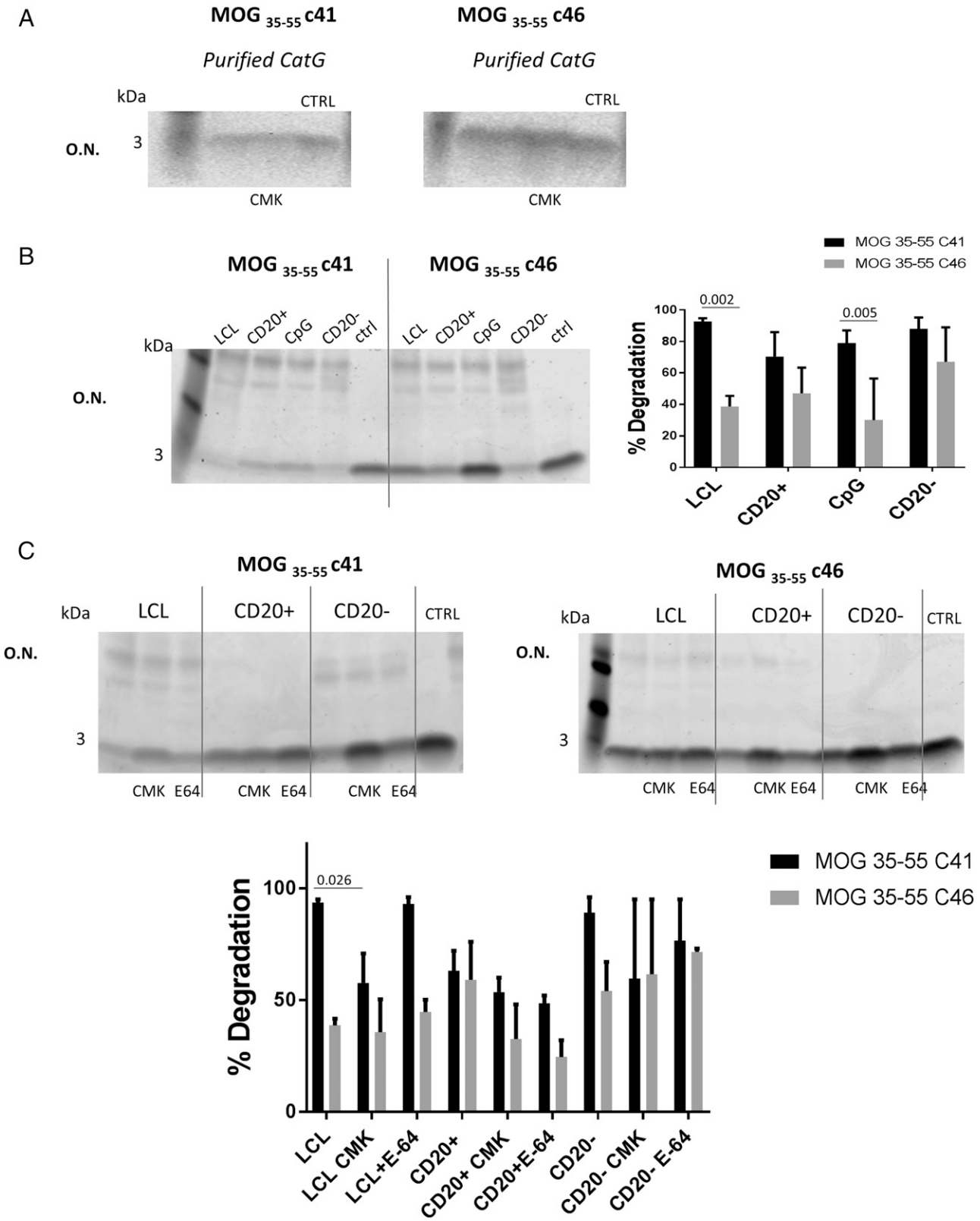

FIGURE 4. Citrullination in p46 protects $MOG_{35–55}$ from degradation by B-LCL. $MOG_{35–55}$ was synthetized whereas the Arg at positions 41 or 46 were replaced by Cit. (**A** and **B**) The peptides $MOG_{35–55}$Cit41 and $MOG_{35–55}$Cit46 were incubated ON with (A) purified human CatG with or without CMK and (B) with B-LCL, isolated $CD20^+$, CpG–activated $CD20^+$, and $CD20^-$ cells. (**C**) The citrullinated peptides were also incubated with B-LCL, $CD20^+$, and $CD20^-$ cells with or without CMK and E64 ON. The right panel of (B) and the bottom panel of (C) show the mean with SEM of percentage degradation of $MOG_{35–55}$Cit41 and $MOG_{35–55}$Cit46 after ON incubation in independent experiments calculated as described in *Materials and Methods* (n = 4, paired repeated-measure two-way ANOVA).

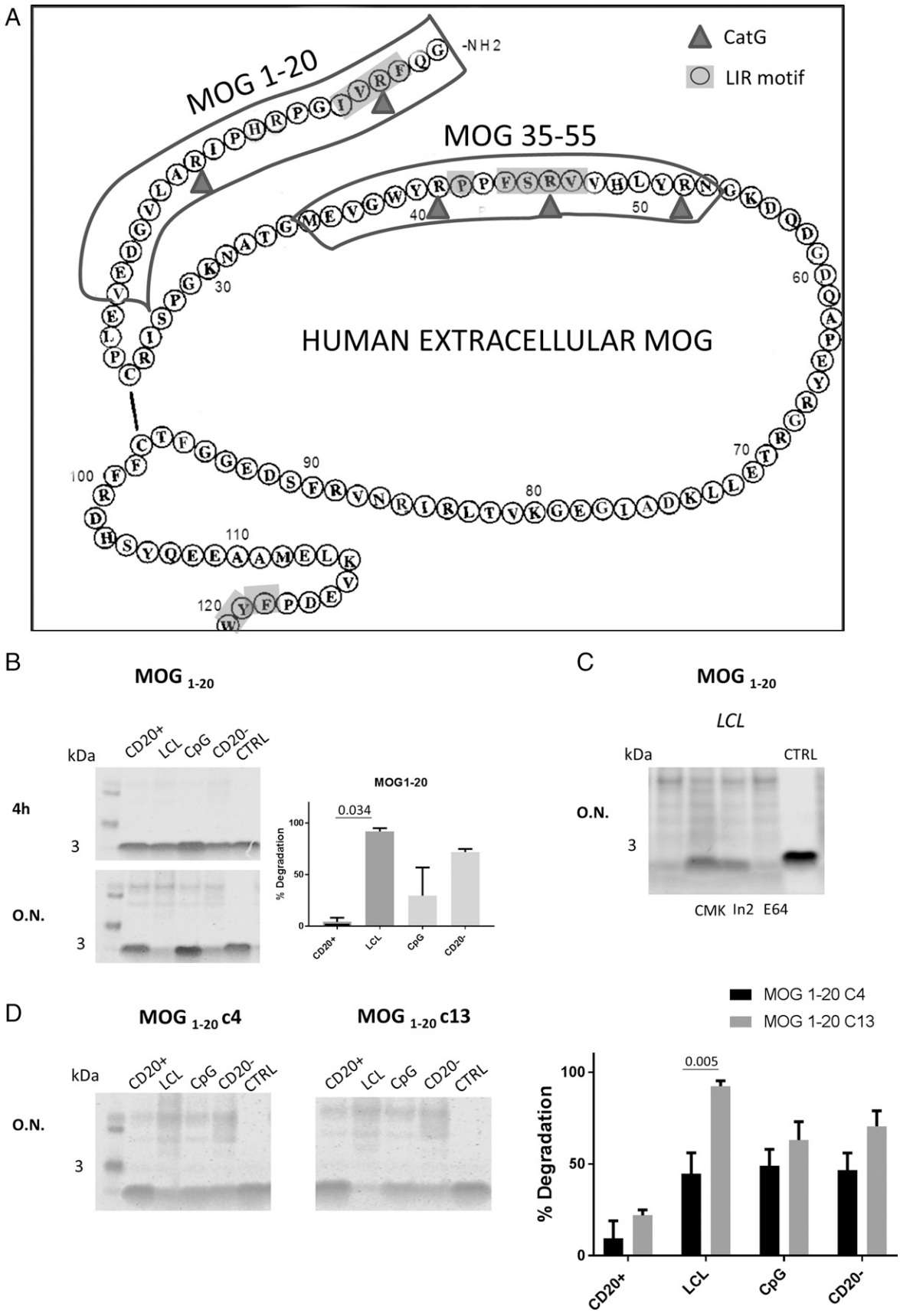

FIGURE 5. Citrullination in LIR motif protects from degradation. (**A**) Sequence of human extracellular MOG protein. The two T cell epitopes $MOG_{35–55}$ and $MOG_{1–20}$ are underlined in boxes with the insertion of CatG cleavage sites (Δ) and LIR motif (O). (**B**) $CD20^+$, B-LCL, CpG–activated $CD20^+$, $CD20^-$ cells have been incubated with $MOG_{1–20}$ for 4 h or ON. The right panel shows the mean with SEM of percentage degradation of $MOG_{1–20}$ after ON incubation in independent experiments (n = 3, paired nonparametric Friedman test). (**C**) B-LCL were incubated ON with $MOG_{1–20}$ with or without CMK, In2, or E64. (**D**) $MOG_{1–20}$ was synthetized whereas the Arg at positions 4 or 13 were replaced by Cit. The peptides $MOG_{1–20}$Cit4 and $MOG_{1–20}$Cit13 (*Figure legend continues*)

$MOG_{34–56}$ peptide harbors the $MOG_{40–48}$ epitope of autoaggressive effector memory $CD8^+CD56^+$ CTL, which mediates a novel pathogenic mechanism leading to progressive disease (20, 21).

We first analyzed the binding and uptake of rhMOG by B-LCL. After 1, 3, 6 h, and ON (16–20 h) incubation, surface and intracellular MOG were measured by FC using the 8-18C5 anti-MOG Ab that only recognizes a conformational epitope, which is formed by the apical B–C, F–G, C'C" loops (22). After incubation we could detect MOG on the B-LCL surface and inside the cells (Fig. 2A). Extracellular staining reached a peak at 1 h and decreased thereafter, suggesting that the Ag is ingested by the B cells (Fig. 2A, upper panels; 2B). Intracellular MOG detection already increased within 1 h, from 1.74 to 22.4% although the fluorescence intensity was lower than the extracellular measurement, suggesting protein degradation, although it may be due to the use of permeabilization reagents. The amount of staining cells increased to 23.5% at the 3 h time point and decreased afterward to the background level in the ON incubation (Fig. 2A, lower panels; 2B).

Blockade of the Fcγ receptor did not significantly reduce either surface or intracellular staining (Fig. 2C), indicating that the observed effects were not due to MOG captured in immune complexes. An increased expression of CD80 (Fig. 2D, 2E), but not CD40 and CD86 (Supplemental Fig. 3), after 1 h incubation suggested a modest increasing effect of rhMOG on the expression of markers relevant for Ag presentation.

We then analyzed rhMOG degradation by the different cell groups to study whether EBV infection has a specific effect on processing of the protein by B cells. rhMOG was incubated for 4 h and ON with the different cell groups, after which degradation was analyzed on SDS gel and quantified. Fig. 2F shows intact rhMOG as a single band of ~14 kDa (Fig. 2F, CTRL line). In primary $CD20^+$ and $CD20^-$ cells, high degradation of rhMOG was detected after 4 h and ON incubation; in CpG-activated B cells and B-LCL, a lower degree of degradation was observed (Fig. 2F). Controls are presented showing a gel with only cells with no MOG (Fig. 2G) and also only B-LCL with or without rhMOG (Fig. 2H).

These data indicate that EBV infection and activation with CpG may reduce the proteolytic degradation of rhMOG by human B cells.

Next, we tested the proteolytic degradation of the immunodominant $MOG_{35–55}$ peptide, a human T cell epitope that can induce EAE in mice as well as NHP (21, 23). The peptide, which is demonstrated in the gel as a 3 kDa band (Fig. 2I, CTRL line), was completely degraded by B-LCL, and to a lesser extent by $CD20^-$ cells, CpG-activated $CD20^+$ cells, and unstimulated B cells (Fig. 2I).

These results suggest that EBV infection of B cells may lead to modifications in MOG processing, thereby rescuing rhMOG from major degradation, but allowing B cells to degrade $MOG_{35–55}$ more effectively (destructive peptide processing).

EBV increases degradation of $MOG_{35–55}$ by B cells through CatG

Cathepsins are a family of endocytic proteases with different substrate specificity and tissue distribution. They are grouped in cysteine (CatB, C, F, H, L, S, V, X, and AEP), serine (CatG and A), and aspartate (CatD and E) cathepsins, and are differentially expressed by specific types of APC. Protease-determined models of Ag processing suggest that cell-specific proteolytic activity can unlock protein Ags by conformational effects on whole proteins as well as generate immunodominant peptides (24). Such processes have important implications for the activation of Ag-specific T cells by APC. In the rhesus macaque and the marmoset, we previously showed that CatG destroys the pathogenic $MOG_{40–48}$ epitope in lysates of LCV-infected B cells. In this study, we tested the hypothesis that EBV has the same effect in intact human B cells.

We fed rhMOG and $MOG_{35–55}$ to the different cell types in the presence or absence of cathepsin inhibitors: CMK as specific CatG inhibitor and E64 as cysteine cathepsin inhibitor. In B-LCL, $CD20^+$, and $CD20^-$ cells CMK inhibits the degradation of rhMOG (Fig. 3A) and $MOG_{35–55}$ (Fig. 3B), whereas E64 does not have any major effect. Controls are presented showing a gel with only cells with or without CMK (Fig. 3C). These results indicate that in all cell types analyzed, the serine protease CatG is leading the degradation of MOG or $MOG_{35–55}$.

A different CatG inhibitor, $C_{36}H_{33}N_2O_6P$ (In2), also protected $MOG_{35–55}$ from total degradation after ON incubation with B-LCL (Fig. 3D). In addition, both CMK and In2 rescued rhMOG and $MOG_{35–55}$ from degradation induced by purified human CatG after ON incubation (Fig. 3E).

We and others (12, 25) showed that B cells and B-LCL do not express CatG mRNA. CatG is mainly produced by neutrophils, but can be internalized by other cells (such as primary monocytes, B cells, dendritic, and murine microglia), probably in an inactive form, through a thrombin-like cell-surface receptor. To test the hypothesis that EBV infection increased CatG activity in B cells, we examined the lysates of different cell types using protease-specific assays. After ON incubation, CatG activity was higher in B-LCL than in $CD20^+$, CpG-activated $CD20^+$, and $CD20^-$ cells (Fig. 3F). Such activity was concentration-dependent, increased over time, and was inhibited by CMK (Fig. 3G).

These data suggest that EBV induces CatG activation leading to degradation of $MOG_{35–55}$.

Citrullination of $MOG_{35–55}$ in position 46 rescues the peptide from degradation

The CatG active site comprises aspartate, histidine, and serine residues, and hydrolyzes peptide bonds near aromatic and strongly positively charged residues (F, K, R, or L) in the P1 position (26). The core 40–48 epitope of the human $MOG_{35–55}$ peptide contains four potential CatG cleavage sites (YRPPFSRVV): the two positively charged Arg residues at position 41 and 46 and the aromatic residues Tyr (Y40) and Phe (F44). To test the hypothesis that substitution of Arg41 or Arg46 by neutrally charged Cit would affect the degradation of $MOG_{35–55}$ by CatG, we incubated $MOG_{35–55}$Cit41 and $MOG_{35–55}$Cit46 with purified CatG ON. We observed complete protection from degradation (Fig. 4A).

We then incubated $MOG_{35–55}$Cit41 and $MOG_{35–55}$Cit46 with B-LCL, $CD20^+$ cells, CpG-activated $CD20^+$ cells, and $CD20^-$ cells. After ON incubation, the Arg41Cit substitution did not alter the sensitivity of the peptide to degradation. By contrast, the Arg46Cit substitution protected the peptide from degradation by B-LCL and CpG-activated $CD20^+$ cells (Fig. 4B). As expected, the CatG inhibitor CMK reduced the degradation of $MOG_{35–55}$Cit41 by B-LCL and $CD20^-$ cells (Fig. 4C).

were incubated ON with $CD20^+$, B-LCL, CpG–activated $CD20^+$, and $CD20^-$ cells. The right panel shows the mean with SEM of percentage degradation of $MOG_{1–20}$Cit4 and $MOG_{1–20}$Cit13 after ON incubation in independent experiments calculated as described in *Materials and Methods* (n = 3, paired repeated-measure two-way ANOVA).

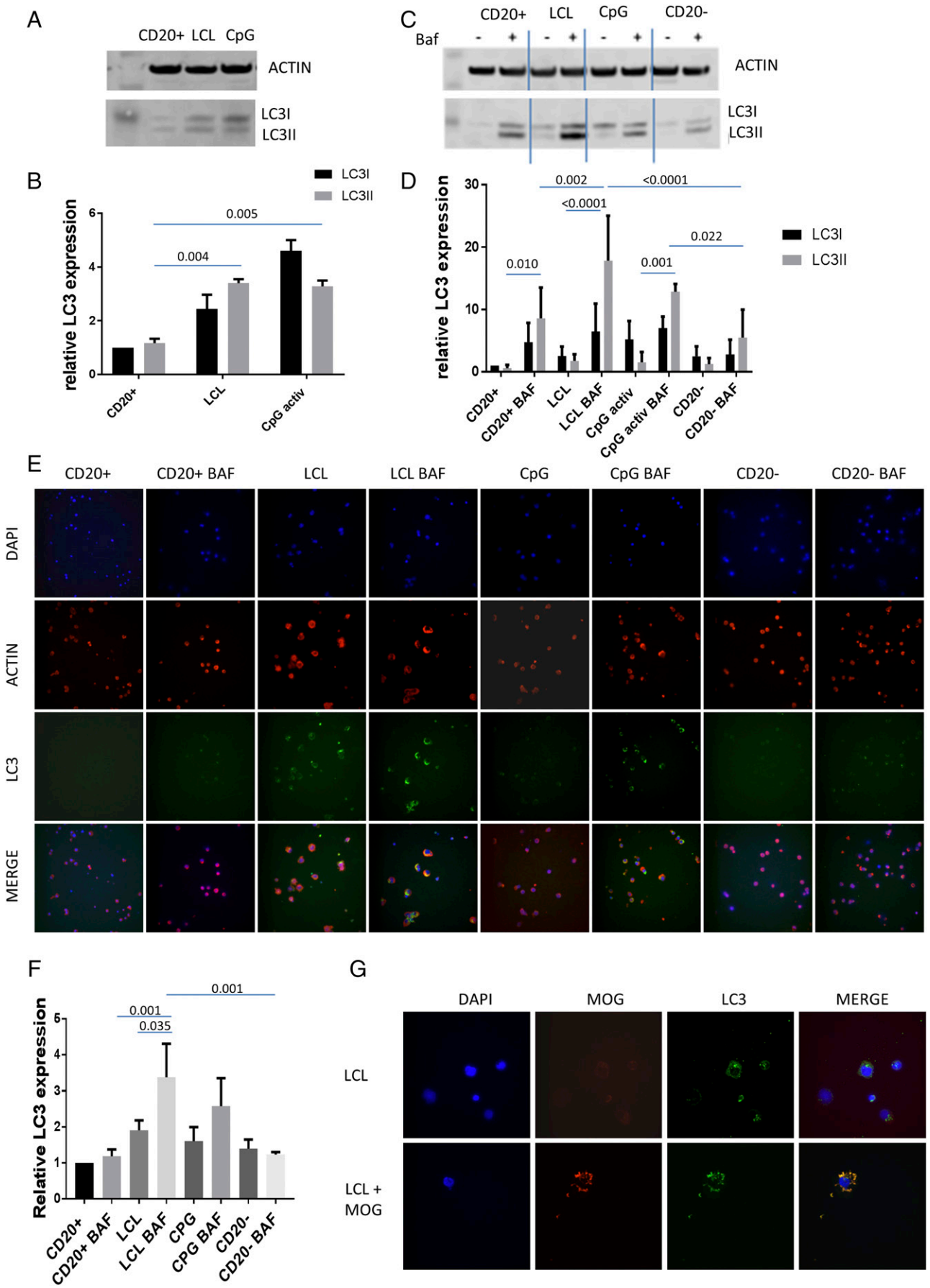

FIGURE 6. EBV infection induces autophagosomes and there is colocalization with rhMOG. (**A**) Indicated cell lysates were immuno-blotted for LC3 and actin as a house-keeping gene product, and (**B**) the density of the LC3-I and LC3II bands were quantified, corrected for the (*Figure legend continues*)

Together, these data show that the Arg to Cit46 substitution makes $MOG_{35–55}$ resistant to proteolytic degradation by B-LCL, whereas citrullination of the Arg41 residue seems to have no effect.

Critical role of LIR motif citrullination in protection of MOG peptides from processing

In our previous studies in NHP, we showed that the Arg46 residue is part of a putative LIR motif in marmoset $MOG_{35–55}$ and that the citrullination of this residue protected the LIR motif from degradation in LCV-infected B cells (12). The microtubule-associated LC3, in particular the phosphatidylethanolamine-linked isoform LC3-II, is expressed on the double membrane of the autophagosome and serves as a docking molecule for proteins targeted for degradation.

The consensus sequence of LIR motifs is [W/Y/F]xx[L/I/V], where x can be any amino acid (27). In the case of an F-LIR core motif, the presence of an acidic residue (E, D, S, T) close to the N-terminal site of the LIR motif is important for stabilization of the relatively weak interaction between F-LIR and LC3-II. We scanned the rhMOG sequence and found three potential LIR motifs: residues 3–6 (FRVI), 44–47 (FSRV), and 118– 122 (FYWV) (Fig. 5A). The Arg46 residue is located in the ^{44}FSRV^{47} LIR motif of $MOG_{35–55}$. We hypothesized that protection of an LIR motif against cleavage by CatG via citrullination would permit binding to LC3-II and association with the autophagosome. We tested this hypothesis in further processing experiments together with another immunodominant MOG peptide, i.e., $MOG_{1–20}$, which contains a putative F-LIR motif in residues 3–6 (FRVI) (Fig. 5A). Similar to $MOG_{35–55}$, this peptide was totally degraded in B-LCL and $CD20^-$ cells after ON incubation (Fig. 5B). CMK and In2 protected $MOG_{1–20}$ from degradation by B-LCL, demonstrating a leading role of CatG in the processing of this peptide (Fig. 5C). Next, we tested the effect of citrullination of Arg4 and 13 in $MOG_{1–20}$ (Fig.5D). Again substitution of Arg4 by Cit, which is located within the F-LIR motif, protected the peptide from the degradation by all cell types, whereas Arg13 substitution did not (Fig. 5D).

Together, these data show that in both $MOG_{35–55}$ and $MOG_{1–20}$, citrullination of the Arg residue within an LIR motif rescues the peptide from degradation, suggesting a role for the autophagosome in their processing.

EBV induces autophagosomes in B cells

Next, we studied the effect of EBV on LC3-II expression as a marker of autophagy. Higher expression of LC3-II was detected in B-LCL as well as CpG-activated B cells (Fig. 6A, 6B). Treatment with BAF (an inhibitor of the fusion between autophagosomes and lysosomes) further increased LC3-II levels in EBV-infected cells assessed by Western blot and immunofluorescence (Fig. 6C–F). This suggests that the rate of LC3-II formation is higher in B-LCL and in CpG-activated B cells compared with other cell types. Immunofluorescence demonstrates colocalization of rhMOG and LC3 after incubation of B-LCL with rhMOG for 1 h at 37° (Fig. 6G), indicating the internalization of rhMOG by B-LCL and its translocation inside autophagosomes.

Induction of autophagy in B-LCL further protects citrullinated MOG peptides from degradation

To further explore the role of autophagy in MOG processing, we treated B-LCL with RAP (an inhibitor of mTOR signaling and activator of autophagy), BAF, or 3-MA (an inhibitor of phagophore formation) (Fig. 7A). LC3-II expression was detected by Western blot as a marker of the autophagy flux. As expected, treatment of B-LCL with RAP and BAF led to increased levels of LC3-II, due to its increased expression and accumulation, respectively. We found that 3-MA had modest effects (Fig. 7B). Next, we incubated B-LCL treated with the above-mentioned stimuli with $MOG_{35–55}$, $MOG_{35–55}$Cit41, $MOG_{35–55}$Cit46, $MOG_{1–20}$, $MOG_{1–20}$Cit4, $MOG_{1–20}$Cit13 (Fig. 7C–J). The key finding was that RAP treatment further reduced degradation of the citrullinated peptides $MOG_{35–55}$Cit46 (Fig. 7E, 7F) and $MOG_{1–20}$Cit4 (Fig. 7H, 7J), suggesting that stimulation of autophagy enhances the protection of peptides with a CatG-resistant LIR motif from degradation in B-LCL.

Discussion

The association of remote EBV infection with increased susceptibility to MS is well established (8). The mechanisms underlying this association, however, have not been clearly elucidated. In this study, we propose that EBV alters the ability of B cells to process and present a pathogenetically relevant myelin autoantigen in a way that leads to autoimmunity. Specifically, EBV infection of B cells endows them with the capacity to cross-present a proteolysis-sensitive epitope of MOG to strongly pathogenic $CD8^+CD56^+$ T cells in the context of MHC-E molecules (20). MOG is a crucial myelin component for the establishment of chronic neuroinflammation in NHP and, potentially, in humans (28).

The success of anti-CD20 treatments in MS underscores the key role of B cells as APC in the disease. The B cells of MS patients are thought to express higher levels of costimulatory molecules than healthy controls (29–31), suggesting an enhanced APC function of B cells in MS. In the marmoset EAE model, considered by many as the closest to the human disease, the pathogenic $CD20^+$ B cells are those infected by LCV, suggesting that the virus could have a critical role in inducing autoimmunity. In this study, we show that EBV infection of human B cells leads to upregulation of HLA class I (A, B, C, and E) and II (DR, DP, and DQ) molecules, as well as the costimulatory molecules CD86, CD40, CD80, and CD70. This increased expression, combined with the previously documented induction of immunoproteasome elements, indicates the activation of the cross-presentation machinery (12, 32). Our studies in the marmoset EAE model indicate that CD80 and CD70 mediate the cross-talk of LCV-infected B cells and autoagressive $MOG_{34–56}$ specific CTLs (33). We speculate that our findings in human B cells (Fig. 1) may reflect similar mechanisms of relevance to the pathogenesis of MS.

The finding that stimulation of B lymphocytes with CpG leads to upregulation of CD40, CD80, and CD86 are supported by previous reports (34–36). Together, our data emphasize that both

background, and means of relative expression of $n = 3$ experiments were plotted in the graph. (**C–F**) Autophagy activity was detected in cells cultured with or without BAF. (C) Indicated cell lysates were immuno-blotted for LC3 and actin as house-keeping gene product, and (D) the density of the LC3-I and LC3II bands were quantified, corrected for the background, and means of relative expression to $CD20^+$ cells of $n = 3$ experiments were plotted in the graph. (E) Cells were stained for immunofluorescence with anti-actin (red) and anti-LC3 (green) and representative images of three independent experiments are shown for cells treated or not treated with BAF. (F) Bar chart represents the mean of the relative quantification of LC3 in cells with or without BAF in $n = 3$ independent experiments ($n = 3$, one-way ANOVA) calculated as described in *Materials and Methods*. (**G**) B-LCL were incubated 1 h with or without MOG and stained for immunofluorescence with anti-MOG (red) and anti-LC3 (green). Original magnification ×400.

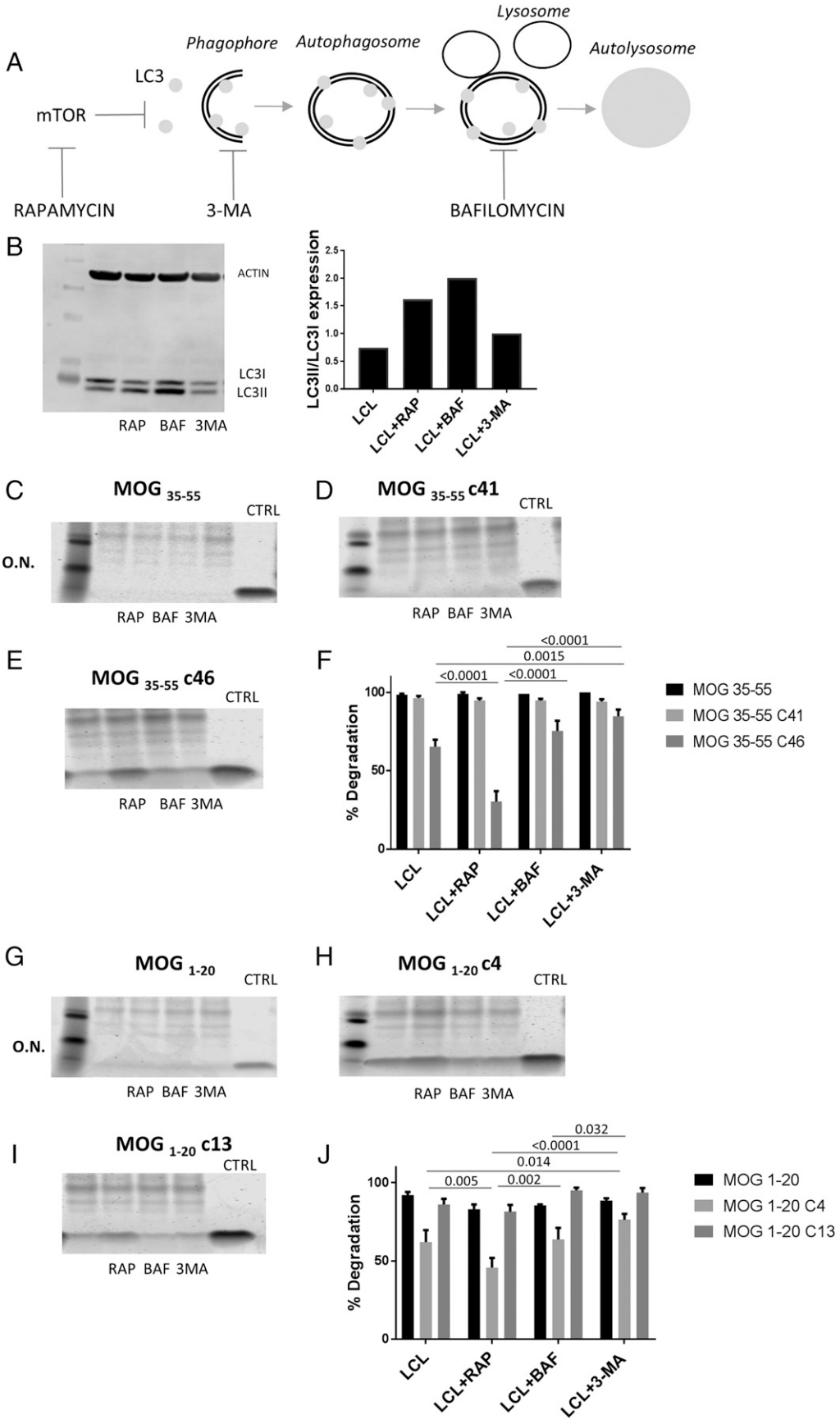

FIGURE 7. Autophagy is directly involved in MOG processing. (**A**) B-LCL were treated with RAP, BAF, and 3-MA. (**B**) Autophagy activity was detected through Western blotting. Treated B-LCL were immuno-blotted for LC3 (left part), and the density of the LC3-I and LC3II bands were quantified, corrected for the background, and the ratio LC3II/LC3I was plotted in the graph (right part). Treated B-LCL were incubated ON with the peptides (**C**) $MOG_{35–55}$, (**D**) $MOG_{35–55}$Cit41, (**E**) $MOG_{35–55}$Cit46, and (**G**) $MOG_{1–20}$, (**H**) $MOG_{1–20}$Cit4, and (**I**) $MOG_{1–20}$Cit13. The panels (*Figure legend continues*)

EBV infection and CpG activation (16) can render B cells as more potent APC and, specifically, able to cross-present exogenous Ags in an MHC class I–restricted manner, although several differences between the two types of activated B cells were found. Although the percentage of cells with an upregulation of costimulatory molecules CD40 and CD86 was comparable, the expression level per cell differed markedly. Moreover, it was only in B-LCL that we observed strong induction of CD70, CD80, and HLA-E, both in cell frequency as well as the expression level per cell (Fig. 1). Finally, CpG activation of B cells does not activate CatG, therefore MOG peptides are less degraded than in B-LCL. These data extend our recent observation of T cell activation mechanisms induced by LCV infection of NHP B cells (12).

We then focused on the subsequent steps of Ag processing, i.e., binding, internalization, and breakdown of Ag. After incubation of B-LCL with rhMOG, we observed its binding to the cell surface as well as its internalization. These two processes peaked at 1 and 3 h, respectively, followed by a rapid reduction in detectable protein. During this process the conformational B cell epitope remains initially intact, as could be deduced from the binding of the 8-18C5 anti-MOG Ab. It is likely that reduced surface staining reflects internalization, whereas reduced intracellular staining reflects degradation of the conformational epitope (22). However, after 1 h of incubation, a proportion of rhMOG with the conformational epitope detected with the 8-18C5 epitope intact could be detected in autophagosomes. The increased expression of CD80 after 1 h suggests simultaneous activation of the Ag presentation machinery during uptake of rhMOG.

Our findings of reduced degradation of rhMOG upon EBV infection of B cells (Fig. 2F) suggest that EBV confers protection from the processing of the whole protein. However, the generation of smaller peptides in the 3–14 kDa range is observed in B-LCL (Figs. 2, 3), but not in $CD20^+$ uninfected B cells, suggesting the breakdown of MOG into 10–20 aa long peptides. The opposite scenario is observed after incubation of the cells directly with the immunodominant peptide $MOG_{35–55}$, with its complete degradation by B-LCL, but not by noninfected and CpG-activated B cells (Figs. 2, 3). Similar to our previous study, we encountered the paradox that the Ag degradation is mediated by CatG even though its mRNA is not expressed in B cells. However, bioactive CatG is identified in the lysate of EBV-infected B-LCL and is likely derived from human serum via receptor-mediated surface binding (37). The inactive form of CatG may be activated by the serine protease activator CatC, the production of which is increased by EBV infection of B cells (12). The current observation that CatG activity in B-LCL increases upon prolonged incubation supports this explanation (Fig. 3G).

The core message of this study is on the role of LCV-induced autophagy in the protection of MOG epitopes against destructive processing. Manoury et al. (24) reported the compelling observation that auto-reactive T cells specific for myelin basic protein (MBP) epitopes that are sensitive to proteolysis by AEP in thymic epithelial cells may escape thymic selection. Activation of these T cells in the periphery is likely prevented by destructive processing of the same epitopes by AEP and/or CatG in B cells (25). In the case of MOG, this tolerogenic function seems to involve a small subset of thymic B cells (38). Our observation in marmosets suggests that B cells in the peripheral immune system may prevent autoaggressive T cell activation by destructive processing of the critical autoantigen epitope $MOG_{40–48}$. EBV infection could convert this tolerogenic mechanism into productive processing of the epitope. The peptide that survives the processing in autophagosomes is then loaded on HLA-E and presented to autoreactive CTLs facilitating autoimmunity (39).

Interestingly, citrullination of just one of the two CatG-targeted Arg residues (position 46, but not 41) protects $MOG_{35–55}$ against degradation. The critical role of the Arg46 residue appears to be its participation in a F-LIR motif, through which the peptide can associate with LC3-II in autophagosomes (27). When this motif is intact, the peptide can associate with autophagosomes, thus prolonging its survival. Nevertheless, lack of association with the autophagosome may lead to degradation of the citrullinated peptide. In line with this concept, we show that increasing the formation of autophagosomes with RAP increases protection of $MOG_{35–55}$. By contrast, inhibition of autophagy with 3-MA enhances its degradation. Of note, the lack of the effect of BAF on peptide processing may be due to its effects being distal to autophagosome formation (Fig. 7). Results obtained with $MOG_{1–20}$ are also consistent with these concepts.

We propose that MOG citrullination is a key peptide modification in the context of autophagy. Indeed, there is increasing evidence that citrullination may play an important role in MS pathogenesis. Increased citrullinated MBP was found in areas of both ongoing and past demyelination in active and chronic active MS lesions, whereas lower levels of citrullinated proteins were observed in control white matter (40). Increased citrullination was also detected in the brains of EAE mice (41). Moreover, HLA-DRB1*15:01 and -DRB5*01:01, which are contained in the HLA-DR2 haplotype that confers the greatest genetic risk for MS, preferentially present peptides that have been citrullinated at key HLA-binding residues (42).

In the animal model it has been reported that citrullinated forms of myelin autoantigen can induce or exacerbate autoimmunity. Citrullinated MBP was highly encephalitogenic in Lewis rats upon active immunization, and adoptive transfer of cMBP-specific T cells led to severe clinical EAE in these animals (43). In mouse EAE, T cells specific for citrullinated MOG peptide transferred into mice with ongoing EAE caused exacerbation of pathology (44). Of note, mice lack an ortholog of EBV-infected B cells. Our previous study showed that infusion of rhesus monkeys with autologous B cells infected with an EBV-related LCV and prepulsed with citrullinated $MOG_{34–56}$ peptide induced autoreactive T cell activation and early signs of encephalitis (10).

To our knowledge, this is the first report that shows the direct implication of autophagy induced by a virus in the processing of autoantigens by human immune cells. Presentation of Ag by resting B cells does not result in immunity activation, but rather in tolerance of the corresponding T cell (45), but when B cells are infected by EBV a different scenario unfolds. In particular, only a small fraction of all B cells ($0.5–300/10^6$ memory B cells) carries the virus (46). Consequently, the difference between the prevalence of MS (affecting ~0.1% of the population) and of EBV infection (60–90% of the population, depending on age and environment), might depend on the fraction of myelin Ag–specific B cell clones that are infected by EBV. These mechanisms are of particular relevance for MS, but may also underlie other autoimmune diseases (47) in which citrullination is involved.

show the mean with SEM of percentage degradation of (**F**) $MOG_{35–55}$, $MOG_{35–55}$Cit41 and $MOG_{35–55}$Cit46, and (**J**) $MOG_{1–20}$, $MOG_{1–20}$Cit4 and $MOG_{1–20}$Cit13 after ON incubation in $n = 3$ independent experiments calculated as described in *Materials and Methods* ($n = 3$, paired repeated-measure two-way ANOVA).

Acknowledgments

We thank Nanci Frakich for technical assistance, Dr. David Onion for FC advice, the Division of Respiratory Medicine for the use of the confocal microscope, Prof. Cris Constantinescu, Dr. Radu Tanasescu, and Prof. Nicola Woodroofe for helpful discussions, Prof. Lindy Durrant and Mohamed Gijon for advice on Western blotting for LC3, Prof. Chris Linington for donating the 8-18C5 anti-MOG antibody, and Dr. Christopher Tench for English proofreading.

Disclosures

The authors have no financial conflicts of interest.

References

1. Hauser, S. L., E. Waubant, D. L. Arnold, T. Vollmer, J. Antel, R. J. Fox, A. Bar-Or, M. Panzara, N. Sarkar, S. Agarwal, et al. 2008. B-cell depletion with rituximab in relapsing-remitting multiple sclerosis. *N. Engl. J. Med.* 358: 676–688.
2. Joseph, F. G., C. L. Hirst, T. P. Pickersgill, Y. Ben-Shlomo, N. P. Robertson, and N. J. Scolding. 2009. CSF oligoclonal band status informs prognosis in multiple sclerosis: a case control study of 100 patients. *J. Neurol. Neurosurg. Psychiatry* 80: 292–296.
3. Serafini, B., B. Rosicarelli, R. Magliozzi, E. Stigliano, and F. Aloisi. 2004. Detection of ectopic B-cell follicles with germinal centers in the meninges of patients with secondary progressive multiple sclerosis. *Brain Pathol.* 14: 164–174.
4. von Büdingen, H. C., A. Palanichamy, K. Lehmann-Horn, B. A. Michel, and S. S. Zamvil. 2015. Update on the autoimmune pathology of multiple sclerosis: B-cells as disease-drivers and therapeutic targets. *Eur. Neurol.* 73: 238–246.
5. Blum, J. S., P. A. Wearsch, and P. Cresswell. 2013. Pathways of antigen processing. *Annu. Rev. Immunol.* 31: 443–473.
6. Pender, M. P. 2003. Infection of autoreactive B lymphocytes with EBV, causing chronic autoimmune diseases. *Trends Immunol.* 24: 584–588.
7. Barcellos, L. F., J. R. Oksenberg, A. J. Green, P. Bucher, J. B. Rimmler, S. Schmidt, M. E. Garcia, R. R. Lincoln, M. A. Pericak-Vance, J. L. Haines, and S. L. Hauser, Multiple Sclerosis Genetics Group. 2002. Genetic basis for clinical expression in multiple sclerosis. *Brain* 125: 150–158.
8. Ascherio, A., and K. L. Munger. 2010. Epstein-barr virus infection and multiple sclerosis: a review. *J. Neuroimmune Pharmacol.* 5: 271–277.
9. Márquez, A. C., and M. S. Horwitz. 2015. The role of latently infected B cells in CNS autoimmunity. *Front. Immunol.* 6: 544.
10. Anwar Jagessar, S., Z. Fagrouch, N. Heijmans, J. Bauer, J. D. Laman, L. Oh, T. Migone, E. J. Verschoor, and B. A. 't Hart. 2013. The different clinical effects of anti-BLyS, anti-APRIL and anti-CD20 antibodies point at a critical pathogenic role of γ-herpesvirus infected B cells in the marmoset EAE model. *J. Neuroimmune Pharmacol.* 8: 727–738.
11. Haanstra, K. G., J. A. Wubben, M. Jonker, and B. A. 't Hart. 2013. Induction of encephalitis in rhesus monkeys infused with lymphocryptovirus-infected B-cells presenting MOG(34-56) peptide. *PLoS One* 8: e71549.
12. Jagessar, S. A., I. R. Holtman, S. Hofman, E. Morandi, N. Heijmans, J. D. Laman, B. Gran, B. W. Faber, S. I. van Kasteren, B. J. Eggen, and B. A. 't Hart. 2016. Lymphocryptovirus infection of nonhuman primate B cells converts destructive into productive processing of the pathogenic CD8 T cell epitope in myelin oligodendrocyte glycoprotein. *J. Immunol.* 197: 1074–1088.
13. 'tHart, B. A., Y. S. Kap, E. Morandi, J. D. Laman, and B. Gran. 2016. EBV infection and multiple sclerosis: lessons from a marmoset model. *Trends Mol. Med.* 22: 1012–1024.
14. Merchant, M., R. Swart, R. B. Katzman, M. Ikeda, A. Ikeda, R. Longnecker, M. L. Dykstra, and S. K. Pierce. 2001. The effects of the Epstein-Barr virus latent membrane protein 2A on B cell function. *Int. Rev. Immunol.* 20: 805–835.
15. Heit, A., K. M. Huster, F. Schmitz, M. Schiemann, D. H. Busch, and H. Wagner. 2004. CpG-DNA aided cross-priming by cross-presenting B cells. *J. Immunol.* 172: 1501–1507.
16. Jiang, W., M. M. Lederman, C. V. Harding, and S. F. Sieg. 2011. Presentation of soluble antigens to CD8+ T cells by CpG oligodeoxynucleotide-primed human naive B cells. *J. Immunol.* 186: 2080–2086.
17. Thorley-Lawson, D. A., and K. P. Mann. 1985. Early events in Epstein-Barr virus infection provide a model for B cell activation. *J. Exp. Med.* 162: 45–59.
18. Livingston, P. G., I. Kurane, and F. A. Ennis. 1997. Use of Epstein-Barr virus-transformed, autologous B-lymphoblastoid cells as antigen-presenting cells for establishment and maintenance of dengue virus-specific, human cytotoxic T lymphocyte clones. *J. Virol. Methods* 67: 77–84.
19. Jagessar, S. A., P. A. Smith, E. Blezer, C. Delarasse, D. Pham-Dinh, J. D. Laman, J. Bauer, S. Amor, and B. 't Hart. 2008. Autoimmunity against myelin oligodendrocyte glycoprotein is dispensable for the initiation although essential for the progression of chronic encephalomyelitis in common marmosets. *J. Neuropathol. Exp. Neurol.* 67: 326–340.
20. Jagessar, S. A., N. Heijmans, J. Bauer, E. L. Blezer, J. D. Laman, N. Hellings, and B. A. 't Hart. 2012. B-cell depletion abrogates T cell-mediated demyelination in an antibody-nondependent common marmoset experimental autoimmune encephalomyelitis model. *J. Neuropathol. Exp. Neurol.* 71: 716–728.
21. Jagessar, S. A., N. Heijmans, E. L. Blezer, J. Bauer, J. H. Blokhuis, J. A. Wubben, J. W. Drijfhout, P. J. van den Elsen, J. D. Laman, and B. A. Hart. 2012. Unravelling the T-cell-mediated autoimmune attack on CNS myelin in a new primate EAE model induced with MOG34-56 peptide in incomplete adjuvant. *Eur. J. Immunol.* 42: 217–227.
22. Breithaupt, C., A. Schubart, H. Zander, A. Skerra, R. Huber, C. Linington, and U. Jacob. 2003. Structural insights into the antigenicity of myelin oligodendrocyte glycoprotein. *Proc. Natl. Acad. Sci. USA* 100: 9446–9451.
23. Adelmann, M., J. Wood, I. Benzel, P. Fiori, H. Lassmann, J. M. Matthieu, M. V. Gardinier, K. Dornmair, and C. Linington. 1995. The N-terminal domain of the myelin oligodendrocyte glycoprotein (MOG) induces acute demyelinating experimental autoimmune encephalomyelitis in the Lewis rat. *J. Neuroimmunol.* 63: 17–27.
24. Manoury, B., D. Mazzeo, L. Fugger, N. Viner, M. Ponsford, H. Streeter, G. Mazza, D. C. Wraith, and C. Watts. 2002. Destructive processing by asparagine endopeptidase limits presentation of a dominant T cell epitope in MBP. *Nat. Immunol.* 3: 169–174.
25. Burster, T., A. Beck, E. Tolosa, V. Marin-Esteban, O. Rötzschke, K. Falk, A. Lautwein, M. Reich, J. Brandenburg, G. Schwarz, et al. 2004. Cathepsin G, and not the asparagine-specific endoprotease, controls the processing of myelin basic protein in lysosomes from human B lymphocytes. *J. Immunol.* 172: 5495–5503.
26. Raymond, W. W., N. N. Trivedi, A. Makarova, M. Ray, C. S. Craik, and G. H. Caughey. 2010. How immune peptidases change specificity: cathepsin G gained tryptic function but lost efficiency during primate evolution. *J. Immunol.* 185: 5360–5368.
27. Birgisdottir, A. B., T. Lamark, and T. Johansen. 2013. The LIR motif - crucial for selective autophagy. *J. Cell Sci.* 126: 3237–3247.
28. Bielekova, B., M. H. Sung, N. Kadom, R. Simon, H. McFarland, and R. Martin. 2004. Expansion and functional relevance of high-avidity myelin-specific CD4+ T cells in multiple sclerosis. *J. Immunol.* 172: 3893–3904.
29. Mathias, A., G. Perriard, M. Canales, C. Soneson, M. Delorenzi, M. Schluep, and R. A. Du Pasquier. 2017. Increased ex vivo antigen presentation profile of B cells in multiple sclerosis. *Mult. Scler.* 23: 802–809.
30. Huang, W. X., P. Huang, and J. Hillert. 2000. Systemic upregulation of CD40 and CD40 ligand mRNA expression in multiple sclerosis. *Mult. Scler.* 6: 61–65.
31. Ireland, S. J., A. A. Guzman, E. M. Frohman, and N. L. Monson. 2016. B cells from relapsing remitting multiple sclerosis patients support neuro-antigen-specific Th17 responses. *J. Neuroimmunol.* 291: 46–53.
32. Cresswell, P., A. L. Ackerman, A. Giodini, D. R. Peaper, and P. A. Wearsch. 2005. Mechanisms of MHC class I-restricted antigen processing and cross-presentation. *Immunol. Rev.* 207: 145–157.
33. Dunham, J., N. van Driel, B. J. L. Eggen, C. Paul, B. A. 't Hart, J. D. Laman, and Y. S. Kap. 2017. Analysis of the cross-talk of Epstein-Barr virus-infected B cells with T cells in the marmoset. *Clin. Transl. Immunol.* 6: e127.
34. Hanten, J. A., J. P. Vasilakos, C. L. Riter, L. Neys, K. E. Lipson, S. S. Alkan, and W. Birmachu. 2008. Comparison of human B cell activation by TLR7 and TLR9 agonists. *BMC Immunol.* 9: 39.
35. Hartmann, G., and A. M. Krieg. 2000. Mechanism and function of a newly identified CpG DNA motif in human primary B cells. *J. Immunol.* 164: 944–953.
36. Decker, T., F. Schneller, T. Sparwasser, T. Tretter, G. B. Lipford, H. Wagner, and C. Peschel. 2000. Immunostimulatory CpG-oligonucleotides cause proliferation, cytokine production, and an immunogenic phenotype in chronic lymphocytic leukemia B cells. *Blood* 95: 999–1006.
37. Yamazaki, T., and Y. Aoki. 1997. Cathepsin G binds to human lymphocytes. *J. Leukoc. Biol.* 61: 73–79.
38. Akirav, E. M., Y. Xu, and N. H. Ruddle. 2011. Resident B cells regulate thymic expression of myelin oligodendrocyte glycoprotein. *J. Neuroimmunol.* 235: 33–39.
39. Camilli, G., A. Cassotta, S. Battella, G. Palmieri, A. Santoni, F. Paladini, M. T. Fiorillo, and R. Sorrentino. 2016. Regulation and trafficking of the HLA-E molecules during monocyte-macrophage differentiation. *J. Leukoc. Biol.* 99: 121–130.
40. Bradford, C. M., I. Ramos, A. K. Cross, G. Haddock, S. McQuaid, A. P. Nicholas, and M. N. Woodroofe. 2014. Localisation of citrullinated proteins in normal appearing white matter and lesions in the central nervous system in multiple sclerosis. *J. Neuroimmunol.* 273: 85–95.
41. Nicholas, A. P., T. Sambandam, J. D. Echols, and S. R. Barnum. 2005. Expression of citrullinated proteins in murine experimental autoimmune encephalomyelitis. *J. Comp. Neurol.* 486: 254–266.
42. Nguyen, H., and E. A. James. 2016. Immune recognition of citrullinated epitopes. *Immunology* 149: 131–138.
43. Cao, L., D. Sun, and J. N. Whitaker. 1998. Citrullinated myelin basic protein induces experimental autoimmune encephalomyelitis in Lewis rats through a diverse T cell repertoire. *J. Neuroimmunol.* 88: 21–29.
44. Carrillo-Vico, A., M. D. Leech, and S. M. Anderton. 2010. Contribution of myelin autoantigen citrullination to T cell autoaggression in the central nervous system. *J. Immunol.* 184: 2839–2846.
45. Raimondi, G., I. Zanoni, S. Citterio, P. Ricciardi-Castagnoli, and F. Granucci. 2006. Induction of peripheral T cell tolerance by antigen-presenting B cells. II. Chronic antigen presentation overrules antigen-presenting B cell activation. *J. Immunol.* 176: 4021–4028.
46. Thorley-Lawson, D. A. 2015. EBV persistence–introducing the virus. *Curr. Top. Microbiol. Immunol.* 390: 151–209.
47. Costenbader, K. H., and E. W. Karlson. 2006. Epstein-Barr virus and rheumatoid arthritis: is there a link? *Arthritis Res. Ther.* 8: 204.